AD-A175 064 NUMERICAL STUDY OF COMPRESSIBLE VISCOUS FLOW BY PSEUDOSPRECTRAL METHOD(U) UNIVERSITY OF SOUTHERN CALIFORNIA LOS ANGELES DEPT OF AEROSPA J C VASSBERG 1/1

UNCLASSIFIED NOV 86 N00014-85-K-2038 F/G 20/4 NL

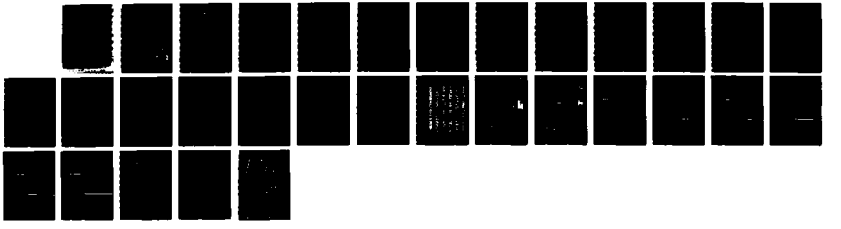

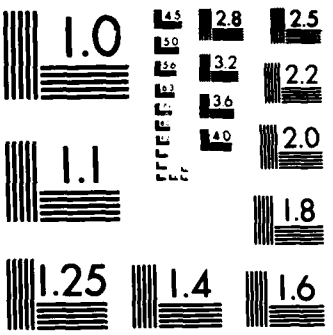

University of Southern California, School of Engineering, Department of Aerospace Engineering, University Park, Los Angeles, CA 90089-0192

Contract N00014-85-K-2038

Title: Numerical Study of Compressible Viscous Flow by Pseudosprectral Method

Date: Nov. 1986

J.C. VASSBERG

1985-1986 RESEARCH

UNIVERSITY OF SOUTHERN CALIFORNIA

DISCLAIMER NOTICE

THIS DOCUMENT IS BEST QUALITY PRACTICABLE. THE COPY FURNISHED TO DTIC CONTAINED A SIGNIFICANT NUMBER OF PAGES WHICH DO NOT REPRODUCE LEGIBLY.

INTRODUCTION

In recent years, an explosion in the capabilities of Computational Fluid Dynamics (CFD) has occured. Since the introduction of the Small Perturbation method of Murman and Cole, transonic CFD has quickly evolved towards Full Potential and Euler methods capable of analyzing a variety of three-dimensional configurations. Although much success has been realized in this field, continued success is inevitable with the ever increasing advances in computing power and faster algorithms. The purpose of this research is to study the applicability of pseudo-spectral schemes for transonic CFD.

MODEL PROBLEMS

Several time-stepping procedures were investigated to become familiar with techniques appropriate for the pseudo-spectral scheme. The procedures were tested on two model problems (including Burgers' inviscid equation), and each procedure's stability criterion was determined. The main purpose of these exercises was to provide the author experience and a sense of confidence in several time-stepping procedures, specifically, their accuracy, and their stability as defined by the mathematical analyses.

The first model problem was to solve a simple differential equation with a known solution for comparison. The differential equation simulated was

$$dy/dt - a*y = \exp(b*t), \text{ with initial condition } y(0) = 1, \qquad (1)$$

where y is a function of t, and a & b are complex constants. The exact solution to equation (1) is

$$y(t) = (1/(b-a))*\exp(b*t) + (1 - 1/(b-a))*\exp(a*t). \qquad (2)$$

The four time-stepping procedures used were Euler's method, a backward method, the mid-point rule, and a leap-frog method. These methods and their stability are discussed below.

Euler's method is a forward-difference scheme which is first-order accurate in time. This scheme is described as

$$Y(n+1) = (1 + a*d)*Y(n) + d*\exp(b*n*d), \qquad (3)$$

where Y is the approximation of y, d is the time step, and n is the time level, ie. t = n*d. A stability analysis of this scheme defines the boundary on the time step as

$$d <= -2*a1/(a1**2 + a2**2), \qquad (4)$$

where a = a1 + i*a2, and i is the square root of -1. Thus, from equation (4) it is easily seen that Euler's method cannot be used if a1 is greater than or equal to 0, or if a2**2 >> abs[a1].

The backward method is a backward-difference scheme which is also first-order accurate in time and is described as

$$(1 - a*d)*Y(n+1) = Y(n) + d*\exp(b*(n+1)*d). \qquad (5)$$

A stability analysis indicates that this scheme becomes more and more stable as the time step goes to infinity. However, since this scheme is only first-order accurate in time, only small time steps should be applied.

The mid-point rule is a second-order time accurate scheme described by

$$(1 - .5*a*d)*Y(n+1) = (1 + .5*a*d)*Y(n) + d*\exp(b*(n+.5)*d). \quad (6)$$

The stability of this scheme requires a1 to be strictly less than 0.

The leap-frog method is also second-order accurate in time and is described as

$$Y(n+1) = Y(n-1) + 2*a*d*Y(n) + 2*d*\exp(b*n*d). \quad (7)$$

Starting the leap-frog scheme also requires an additional unknown, ie. Y(1), which can be approximated using the mid-point rule so that second-order accuracy is maintained. The leap-frog scheme is stable if $d < 1/a1$, thus useless if a1 is negative.

The above time-stepping procedures were tested for a variety of complex constants a & b to verify the stability estimates and order of accuracy determined by the mathematical analyses. With the confidence provided by the first simple model problem, it was time to study an equation with the flavor of a transonic flow problem.

The second model problem investigated was Burgers' inviscid equation. In conservation form, this quasi-linear partial

differential equation is described by

$$du/dt + .5*d(u**2)/dx = 0, \tag{8a}$$

or in quasi-linear form, described by

$$du/dt + u*du/dx = 0. \tag{8b}$$

Let us consider the initial conditions

$$\begin{aligned} u(x,0) &= 0.5, && x < 0, \\ u(x,0) &= 1.25 - \mathrm{sqrt}(0.5625 + 2*x - x**2), && 0 < x < 1, \\ u(x,0) &= 0.0, && 1 < x. \end{aligned} \tag{8c}$$

The initial conditions were chosen such that a "shock" would eventually form in the solution, thus providing a reasonable test case for a scheme to be used for transonic flow calculations. The exact solution to equations (8) is presented and discussed. In addition, several numerical methods are used to calculate approximations for the above problem and are compared to the exact solution through discussion. The numerical methods are analyzed for stability criteria and order of dissipation when applied to a form of equations (8b) with constant coefficients, ie. du/dt + A*du/dx = 0, where u is a vector and A is a constant matrix. The stability criteria used (for approximating the differential equation) is the most restrictive one obtained by allowing the constant A to vary over the interval containing all values of u, ie. [0.0,0.5].

Observe that equation (8b) can be solved using the method of characteristics. Thus, u = u(r,s), where r describes the x-location on the data line where the characteristic line starts and s is in the direction of the characteristic line. Note that at some time, the characteristic lines begin to merge to form a shock. The movement of this discontinuity can be described by the entropy jump condition (see Reference 1). By observation of equation (8b) and initial conditions (8c), it can be noted that a shock will surely form and will travel to the right. The presentation of the exact solution will be given in three parts, specifically, the time before the shock (ie. $0 < t < t1$), during the growth of the shock (ie. $t1 < t < t2$), and after the shock is fully mature (ie. $t2 < t$). Using the method of characteristics, the exact solution for the first time interval can be shown to be

$$\begin{aligned} u(x,t) &= 0.5, && x < t/2, \\ u(x,t) &= u(r,0), && t/2 < x < 1, \\ u(x,t) &= 0.0, && 1 < x, \end{aligned} \tag{9a}$$

where u(r,0) is defined by (8c) and r is given by

$$1.25*t - \mathrm{sqrt}(0.5625 + 2*r - r**2)*t + r - x = 0. \tag{9b}$$

Solutions (9) are valid only on the time interval: $0 <= t <= t1$, where t1 is the time at which the shock first forms. The value of t1 can be determined by finding the first occurrence of abs(du/dx) approaching infinity, ie. when characteristic lines begin to merge

together. These calculations show that the shock begins at $x = 0.375$ and $t = 0.75$, thus defining t1.

The exact solution for the second interval is described by

$$\begin{aligned} u(x,t) &= 0.5, && x < x\text{shock}, \\ u(x,t) &= u(r,0), && x\text{shock} < x < 1, \\ u(x,t) &= 0.0, && 1 < x, \end{aligned} \tag{10}$$

where u(r,0) and r are as before, and xshock is the x-location of the shock. To define the motion of the shock during its growth, a numerical time-stepping procedure was utilized based on conserving properties across the discontinuity. This shock motion is provided in Table I where shock location, r-, r+, u+, and shock speed are provided as a function of time. (Here, the + and - indicate on which side of the shock the property is given.) Note that the shock speed monotonically decreases from 0.5 to 0.25 during its growth. Another important item to note from Table I is the time of shock maturity, which defines t2 to be 2.79533.

The exact solution for the third interval is now known to be described by

$$\begin{aligned} u(x,t) &= 0.5, && x < x\text{shock}, \\ u(x,t) &= 0.0, && x\text{shock} < x, \end{aligned} \tag{11}$$

where $x\text{shock} = 1 + 0.25*(t - t2)$.

The exact solution to Burgers' problem (8) is described by equations (9-11) and is illustrated in Table I and Figures 1-2. Figure 1 provides a solution profile for several "key" times. The first time (t = 0.0) illustrates the initial conditions, the second time (t = t1 = 0.75) indicates the start of the shock, the third & fourth times (t = 1.5 & 2.25) help show the growth of the shock, and the fifth time (t = 2.79533) shows the instant the shock becomes fully mature. Figure 2 illustrates the position of the shock as a function of time. Notice that the shock forms at x = 0.375 and t = t1 = 0.75, and becomes fully mature at x = 1.0 and t = t2 = 2.79533. Also, notice that the solution to the left of the shock and the r = 0 characteristic is u = 0.5, the solution to the right of the mature shock and the r = 1 characteristic is u = 0.0, and the solution in between is determined by equations (9b), (8c), and Table I. With the exact solution of Burgers' equation (8) known, several numerical approaches will be evaluated.

The first numerical approximation to equations (8) uses MacCormack's method (Reference 2). This scheme is second-order accurate, conditionally stable, fourth-order dissipative, and can be split into two steps; a predictor step and a corrector step. For the conservation form (8a), the scheme is described by

$$\begin{aligned} Vtmp(i) &= V(i,n) - q*0.5*(V(i+1,n)**2 - V(i,n)**2) \\ V(i,n+1) &= 0.5*(V(i,n) - q*0.5*(Vtmp(i)**2 - Vtmp(i-1)**2)) \\ &\quad + 0.5*Vtmp(i), \end{aligned} \tag{12a}$$

and for the quasi-linear form (8b), the scheme is described by

$$\begin{aligned} Vtmp(i) &= V(i,n) - V(i,n)*q*(V(i+1,n) - V(i,n)) \\ V(i,n+1) &= 0.5*(V(i,n) - Vtmp(i)*q*(Vtmp(i) - Vtmp(i-1)) \\ &\quad + 0.5*Vtmp(i), \end{aligned} \qquad (12b)$$

where V is the approximation of the exact solution u, Vtmp is a temporary value determined by the predictor step, i indicates the spatial location (ie. x = i*delta-x), n indicates the time level (ie, t = n*delta-t), and q is the ratio of delta-t to delta-x. As mentioned previously, MacCormack's scheme is conditionally stable and through mathematical analyses, stability requires q <= 2.0. Figure 3 illustrates the solution of equations (12a) for initial data (8c) at times of 0, 1, 2, 3, 4, 5, and 6. Notice that the shock is fully mature by time equal to 3.0. (Recall that the exact solution has the first occurrence of a mature shock at time equal to 2.79533.) Also, notice that the mature shock speed is almost exactly equal to 0.25, which compares very nicely with the exact solution. Another item to notice in Figure 3 is that the solution seems to be stable with no pre-shock oscillations evident. This solution was obtained with delta-x = 0.05, and delta-t = 0.10, which by the mathematical analysis is neutrally stable (ie. q = 2.0). Figure 4 shows the solution of equations (12b) for the same time levels. This solution is stable; however, the most important thing to note is that the shock stagnates at x = 1.0. This figure definitely indicates the importance of using the conservation form of Burgers' equation as opposed to using its quasi-linear form. Another item to notice is

that a pre-shock oscillation seems to be forming as the time increases. This solution also used delta-x = 0.05 and delta-t = 0.10.

The second approach used to solve Burgers' problem (8) was an implicit scheme developed by Beam and Warming (Reference 3). This scheme has been analyzed to be neutrally stable and non-dissipative. For convenience, delta-x and delta-t have been chosen to be equal to that used for MacCormack's method. This scheme approximates the conservative form (8a) by,

$$0.25*q*(V(i+1,n)*V(i+1,n+1) - V(i-1,n)*V(i-1,n+1)) + V(i,n+1) = V(i,n), \qquad (13a)$$

and the quasi-linear form (8b) by,

$$V(i,n+1) + 0.5*q*V(i,n)*(V(i+1,n+1) - V(i-1,n+1)) = V(i,n). \qquad (13b)$$

Figure 5 shows the solution of (13a) for times equal to 0.0, 0.5, 1.0, 1.5, and 2.0. Notice the extreme pre-shock oscillations for this solution. This occurs because the Beam-Warming scheme is non-dissipative. The solution to equation (13b), shown in Figure 6, also has the extreme pre-shock oscillation. To remedy this problem, a fourth-order dissipative term is added to the right-hand side of equations (13). This term is explicitly defined as,

$$-0.125*w*(V(i+2,n) + V(i-2,n) - 4*(V(i+1,n) + V(i-1,n)) + 6*V(i,n)) \qquad (14$$

where w determines the amount of dissipation and is allowed to have the values 0 <= w <= 1 according to a linearized stability analysis. Figure 7 shows the solution of equation (13a) with the dissipation term (14) for times of 0.0, 0.5, 1.0, 1.5, 2.0, 2.5, and 3.0 with w equal to 0.75. The dissipation term had very little effect on the pre-shock oscillations when applied to the conservative form (13a), yet damped the oscillations of the quasi-linear form (13b) very nicely as is shown in Figure 8. Also, notice in Figures 7-8 that the dissipation term produced a small oscillation at the base of the shock.

The third approach used to solve Burgers' problem (8) was a pseudo-spectral method. Since the solution to Burgers' inviscid problem with the given initial conditions is obviously non-periodic, a Chebyshev polynomial expansion is employed to evaluate the spatial derivatives in a spectral manner. In particular, the author investigated the space interval (-1,3) for times between 0 and 3. The spatial interval is discreatized with I cells, thus the solution is described by I+1 values at the collocation points. These points are located at,

$$X(i) = S*\cos(pi*i/I) + T \qquad \text{for } i = 0,1,\ldots,I, \qquad (15)$$

where S is a scale parameter, and T is a translation parameter. For the spatial interval investigated, S = 2, and T = 1. The solution at the I+1 points is described by,

$$U(i) = \text{Sum}(j=0,I)\ A(j)*\cos(pi*i*j/I) \qquad \text{for } i = 0,1,\ldots,I, \qquad (16)$$

where the A(j) coefficients can be evaluated by the inverse transform,

$$A(j) = 2/(I*C(j)) * \mathrm{Sum}(i=0,I)\ U(i)*\cos(pi*j*i/I)/C(i), \quad (17)$$

where C(j) = 2 for j = 0 or I, and C(j) = 1 otherwise. Equations (16-17) can be evaluated by Fast Fourier Transforms (FFT) if I is a composite integer. By differentiating equation (16), one obtains,

$$UX(i) = \mathrm{Sum}(j=0,I)\ B(j)*\cos(pi*i*j/I)/S, \quad (18)$$

where B(j) can be computed from A(j) by using the recurrent relations,

$$\begin{aligned} B(I) &= 0, \\ B(I-1) &= 2*I*A(I), \\ B(j) &= (B(j+2) + 2*(j+1)*A(j+1))/C(j). \end{aligned} \quad (19)$$

The time-stepping algorithm used is a simple predictor-corrector scheme, and is described by,

$$\begin{aligned} Utmp(i) &= U(i,n) + k*U(i,n)*UX(i,n), \\ U(i,n+1) &= 0.5*(U(i,n) + k*Utmp(i)*UXtmp(i) + Utmp(i)), \end{aligned} \quad (20)$$

where k is the delta-time specified. Since the solution to equation (8) is discontinuous, spurious oscillations are introduced in the pseudo-spectral scheme such that the scheme inevitably diverges. To

aid convergence, a spectral filter is applied to the A(j) terms to reduce the amplitude of the high frequency contributions. This filtering scheme is given as,

$$A(j) = A(j) \qquad \text{for } j = 0,1,\ldots,J0,$$
$$A(j) = A(j)*\exp(RH0*((j-J0)/(I-J0))**4) \qquad \text{otherwise,} \qquad (21)$$

where RH0 is the decay parameter and J0 is the cut-off filter parameter.

The above pseudo-spectral method was tested on Burgers' equation (8) in both conservative and quasi-linear form. Figure 9 illustrates the pseudo-spectral approximation of Burgers' equation (8a) in conservation form for several times. Notice the growth of the pre-shock oscillations with time. Figure 10 illustrates the solution of the quasi-linear equation (8b) for the same times. Notice that the pre-shock oscillations are more pronounced and the shock movement is slower than the conservative solution. In fact, the quasi-linear shock will stagnate at X = 1, while the conservative shock will continue to move to the right with a speed approximately equal to the exact solution. This behavior between the conservative and quasi-linear solutions has been observed before in the MacCormack and Beam-Warming schemes.

In addition to the above effort, some time was spent studying Fast Fourier Transform algorithms (Reference 4) (which are essential to the economical competitiveness of the spectral schemes), spectral filtering schemes, and artificial dissipation terms (References 5-8) (which are neccessary for shock-capturing when using the spectral methods). After experimenting with these shock-capturing techniques

and examining similar results from other researchers (including those in favor of the pseudo-spectral scheme), it seems that the pseudo-spectral method is very well suited for smooth solutions. However, if the solution contains a discontinuity, the high-order accuracy of the pseudo-spectral scheme can quickly degenerate to as poor as first-order accuracy; easily eliminating any advantage the pseudo-spectral scheme may have over the simpler second-order finite-difference or finite-element schemes. The substantial loss in accuracy of a spectral shock-capturing scheme is verified by Hussaini (Reference 9) when studying the time development of shock waves in a spiral galaxy. In order to retain the high accuracy of the pseudo-spectral method (for solutions with discontinuities), a shock-fitting technique could be employed. The solution discontinuity, by being fitted, could be represented as a boundary, and by using Chebyshev polynomials, one could handle the non-periodic boundary conditions (Reference 10 studies a similar approach). Although this concept would retain the high-order accuracy desired, it would also introduce a new set of problems. These problems include 1) the prohibitively small time steps allowed by the stability of schemes using the Chebyshev spacing, 2) problems handling multiple shocks, and 3) problems expanding the shock-fitting scheme to three-dimensional solutions. In view of the obstacles outlined above, the author feels that the pseudo-spectral scheme is not well suited for "practical" transonic problems.

PROPOSED RESEARCH

The proposed research is to develop a transonic Euler method based on a finite-element scheme similar to that of Jameson et. al. The intention is to develop a flow solver universal to any type configuration regardless of dimension or topology, and initially develop a grid generation and post-processor package for two-dimensional airfoil geometries. Although the flow solver will be very general, the grid generation and flow-solution post-processor packages will be particular to each case, thus future work will include expanding the capability of the method by developing grids for multielement airfoils and three-dimensional configurations. Other items which may be explored are: 1) multigrid, 2) "smart" dissipation at shock locations, 3) code designed for parallel processing, 4) capability for an inverse mode, 5) viscous effects, 6) local mesh refinement, 7) inclusion of power effects, and 8) more general grid generation tools to ease future geometric needs.

CONCLUSIONS

* The pseudo-spectral scheme is excellent for smooth solutions.
* The pseudo-spectral scheme can easily degenerate to first-order accuracy if a discontinuity exists in the solution.
* Spectral-filtering, solution smoothing, and dissipation terms are neccessary to stabilize the pseudo-spectral scheme if a discontinuity is to be "captured".
* Pseudo-spectral schemes are not suited for the general inviscid transonic problem.
* The proposed flow solver will be universal to any geometry, thus reducing uncertanties usually introduced by different flow solvers on different geometries.
* The proposed method will also be set up for time-accurate solutions.
* The triangular/tetrahedral elements of the proposed method will allow the development of very general contour-plotting, streamline tracing, and other post-processing graphics packages.

REFERENCES

1. Lax, P.D., "Hyperbolic Systems of Conservation Laws and the Mathematical Theory of Shock Waves", Vol. 11, Regional Conference Series in Applied Mathematics, 1973, SIAM, Philadelphia.
2. MacCormack, R.W., and Paullay, A.J., "Computational Efficiency Achieved by Time Splitting of Finite Difference Operators", AIAA Paper 69-354, Cincinnati, Ohio, 1969.
3. Warming, R.F., and Beam, R.M., "Upwind Second-Order Difference Schemes and Applications in Aerodynamic Flows", AIAA Journal, Vol. 14., No. 9, Sep. 1976.
4. Cooley, J.W., and Tukey, J.W., "An Algorithm for the Machine Calculation of Complex Fourier Series", Mathematics of Computers, XIX, 1965, pp. 45-51.
5. Gottlieb, D., Hussaini, M.Y., and Orszag, S.A., "Theory and Applications of Spectral Methods", ICASE Report 83-66, Dec. 1983.
6. Sakell, L., "Pseudospectral Solution of Inviscid Flows with Multipule Discontinuities", NRL Memorandum 5147, Aug. 1983.
7. Sakell, L., "Pseudospectral Solutions of One- and Two-Dimensional Flows with Shock Waves", AIAA Journal, Vol. 22, No. 7, July 1984.
8. Ou, Y.R., Private Communications, USC, 1985-1986.
9. Hussaini, M.Y., Kopriva, D.A., Salas, M.D., and Zang, T.A., "Spectral Methods for the Euler Equations: Part I - Fourier Methods and Shock-Capturing", AIAA Journal, Vol. 23, Jan. 1985, pp. 64-70.
10. Hussaini, M.Y., Kopriva, D.A., Salas, M.D., and Zang, T.A., "Spectral Methods for the Euler Equations: Part II - Chebyshev Methods and Shock-Fitting", AIAA Journal, Vol. 23, Jan. 1985, pp. 234-240.

TABLE I

and

FIGURES 1-10

TIME	X	TAU-	TAU+	U+	SHOCK SPEED
0.75000	0.37500	0.00000	0.00000	0.50000	0.50000
0.80000	0.39944	-0.00056	0.03671	0.45340	0.47670
0.85000	0.42275	-0.00225	0.07321	0.41122	0.45561
0.90000	0.44504	-0.00496	0.10991	0.37237	0.43618
0.95000	0.46641	-0.00859	0.14650	0.33674	0.41837
1.00000	0.48692	-0.01308	0.18278	0.30414	0.40207
1.05000	0.50666	-0.01834	0.21858	0.27436	0.38718
1.10000	0.52568	-0.02432	0.25378	0.24718	0.37359
1.15000	0.54405	-0.03095	0.28828	0.22240	0.36120
1.20000	0.56183	-0.03817	0.32202	0.19984	0.34992
1.25000	0.57907	-0.04593	0.35494	0.17930	0.33965
1.30000	0.59582	-0.05418	0.38699	0.16063	0.33032
1.35000	0.61212	-0.06288	0.41817	0.14367	0.32183
1.40000	0.62802	-0.07198	0.44845	0.12826	0.31413
1.45000	0.64355	-0.08145	0.47784	0.11429	0.30714
1.50000	0.65875	-0.09125	0.50633	0.10161	0.30081
1.55000	0.67365	-0.10135	0.53394	0.09013	0.29507
1.60000	0.68828	-0.11172	0.56068	0.07974	0.28987
1.65000	0.70265	-0.12235	0.58658	0.07035	0.28517
1.70000	0.71680	-0.13320	0.61164	0.06186	0.28093
1.75000	0.73076	-0.14424	0.63590	0.05420	0.27710
1.80000	0.74452	-0.15548	0.65937	0.04731	0.27365
1.85000	0.75813	-0.16687	0.68209	0.04110	0.27055
1.90000	0.77159	-0.17841	0.70407	0.03553	0.26777
1.95000	0.78491	-0.19009	0.72534	0.03055	0.26527
2.00000	0.79812	-0.20188	0.74594	0.02609	0.26305
2.05000	0.81123	-0.21377	0.76587	0.02212	0.26106
2.10000	0.82423	-0.22577	0.78518	0.01860	0.25930
2.15000	0.83716	-0.23784	0.80387	0.01548	0.25774
2.20000	0.85001	-0.24999	0.82198	0.01274	0.25637
2.25000	0.86280	-0.26220	0.83953	0.01034	0.25517
2.30000	0.87553	-0.27447	0.85653	0.00826	0.25413
2.35000	0.88822	-0.28678	0.87302	0.00647	0.25323
2.40000	0.90086	-0.29914	0.88901	0.00494	0.25247
2.45000	0.91347	-0.31153	0.90452	0.00365	0.25183
2.50000	0.92605	-0.32395	0.91957	0.00259	0.25130
2.55000	0.93860	-0.33640	0.93418	0.00173	0.25087
2.60000	0.95113	-0.34887	0.94836	0.00107	0.25053
2.65000	0.96365	-0.36135	0.96213	0.00057	0.25029
2.70000	0.97616	-0.37384	0.97552	0.00024	0.25012
2.75000	0.98867	-0.38633	0.98852	0.00005	0.25003
2.79533	1.00000	-0.39766	1.00000	0.00000	0.25000

TABLE I: "Tabulated Characteristics of the Propogating Shock during its growth from birth to maturity."

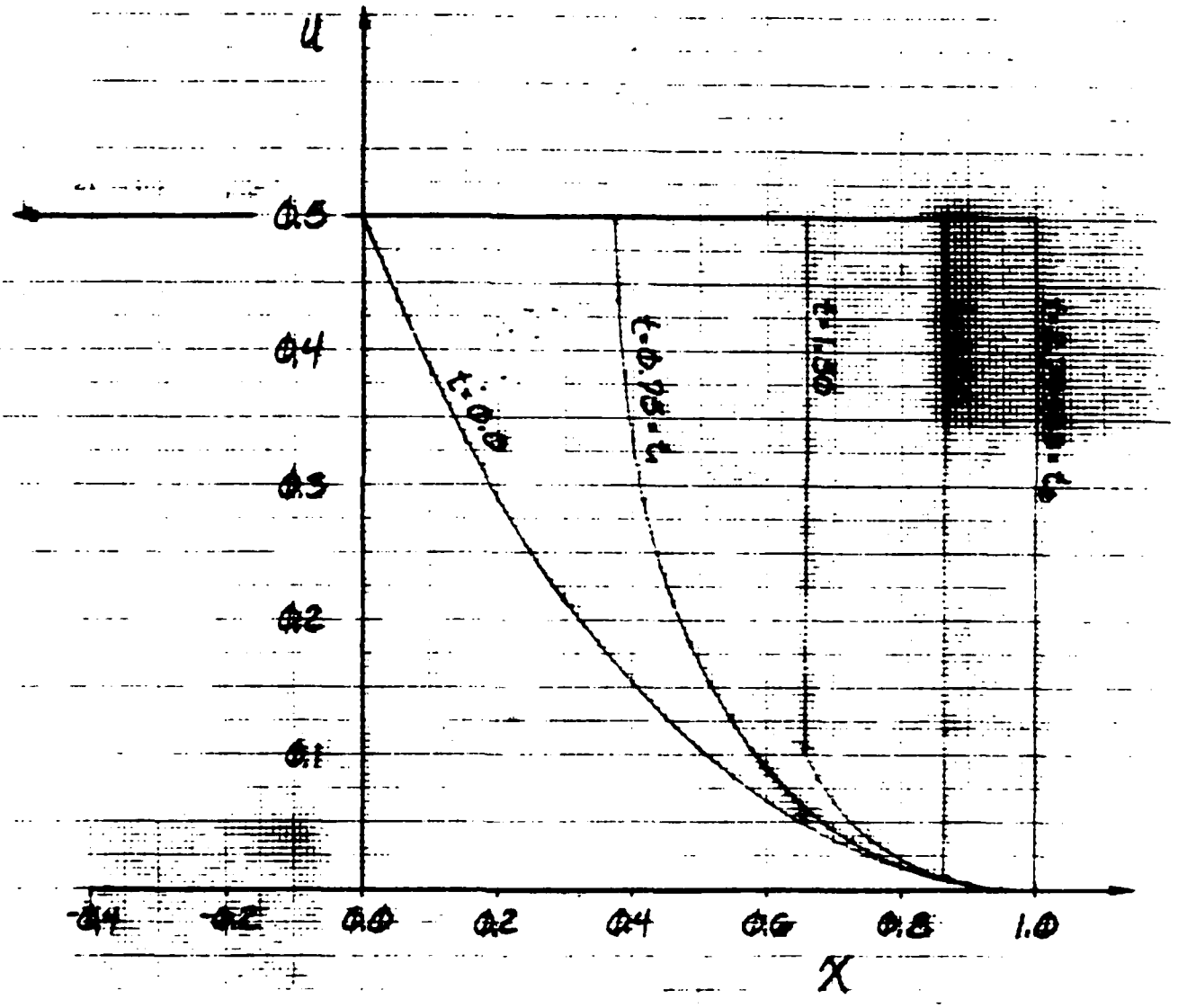

FIGURE 1: "Exact Solution of Burgers' equation for the shown Initial Data at several different times."

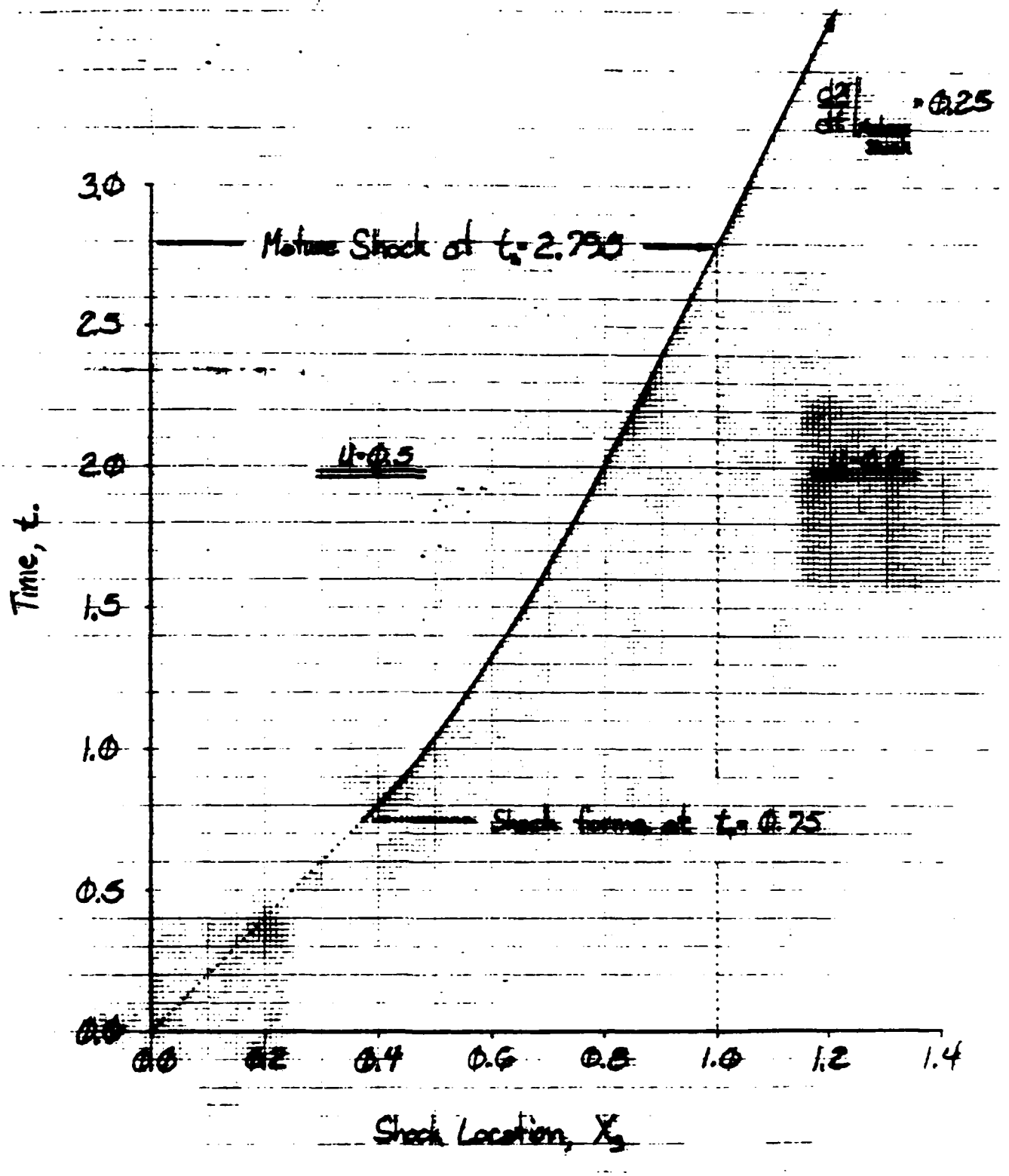

FIGURE 2: "Shock Location for the Exact Solution of Burgers' equation and Initial Data illustrated in Figure 1."

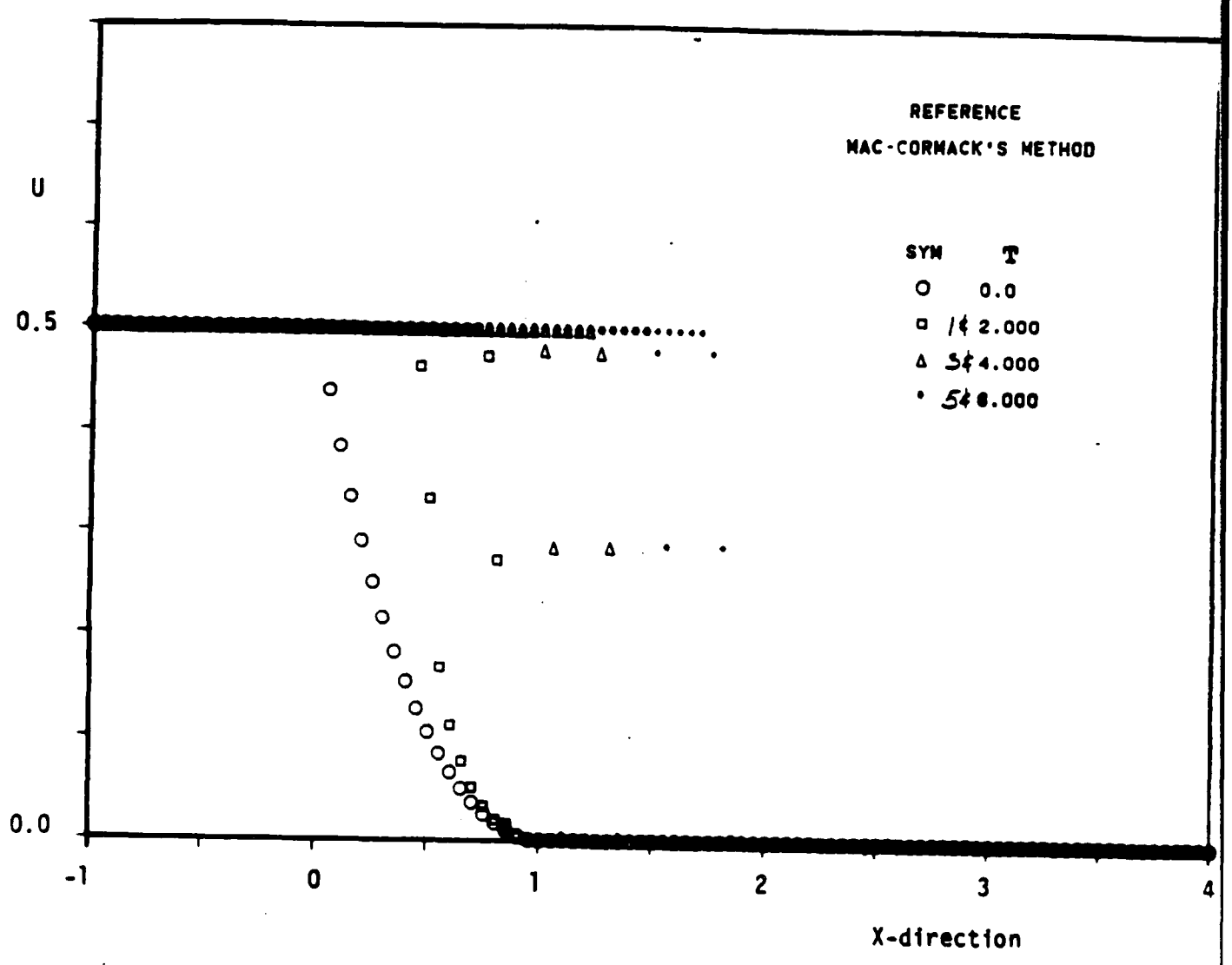

FIGURE 3: "Numerical solution of Burgers' equation in Fully-Conservative form using MacCormack's method."

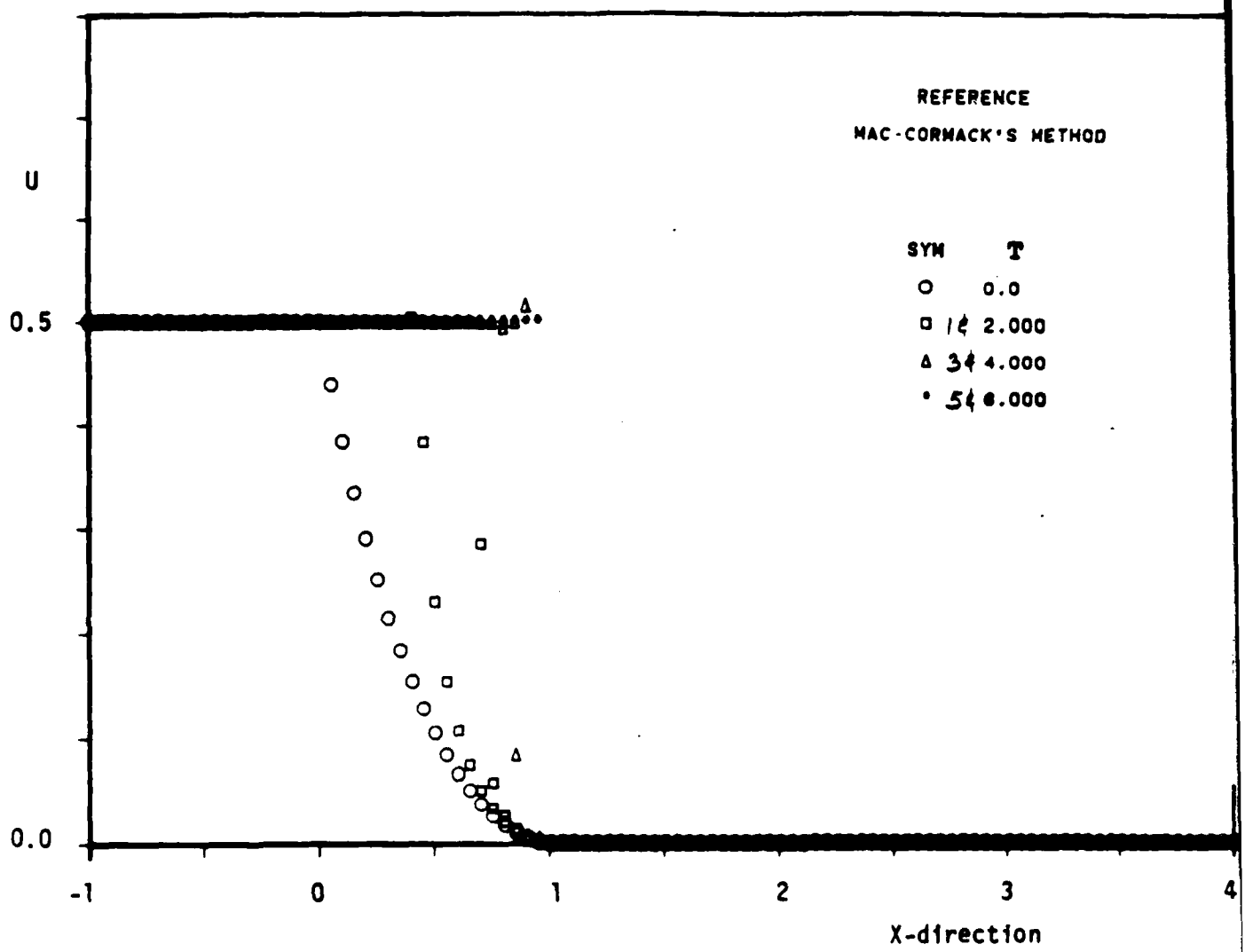

FIGURE 4: "Numerical solution of Burgers' equation in Quasi-Linear form using MacCormack's method."

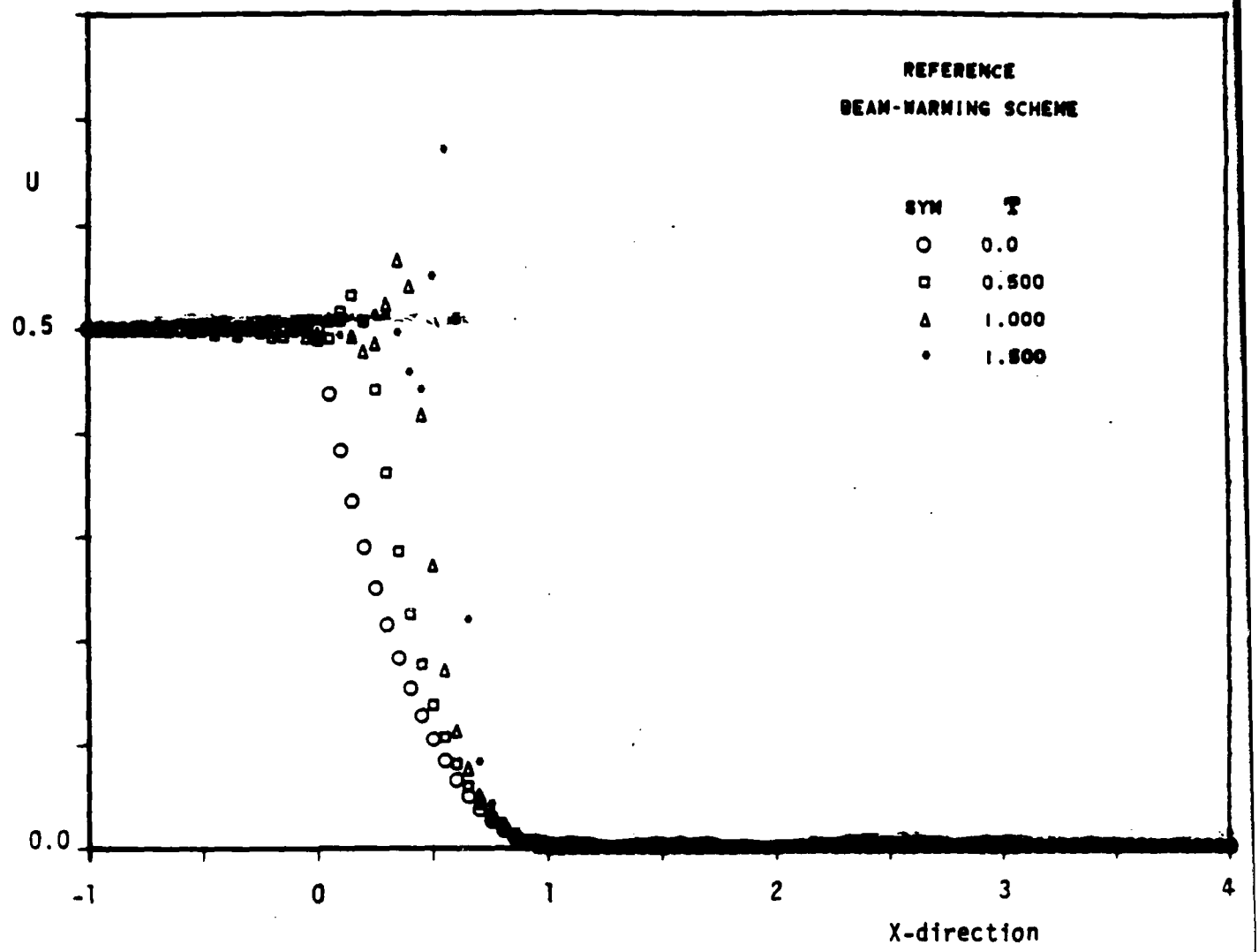

FIGURE 5: "Numerical solution of Burgers' equation in Fully-Conservative form using Beam-Warming's implicit method."

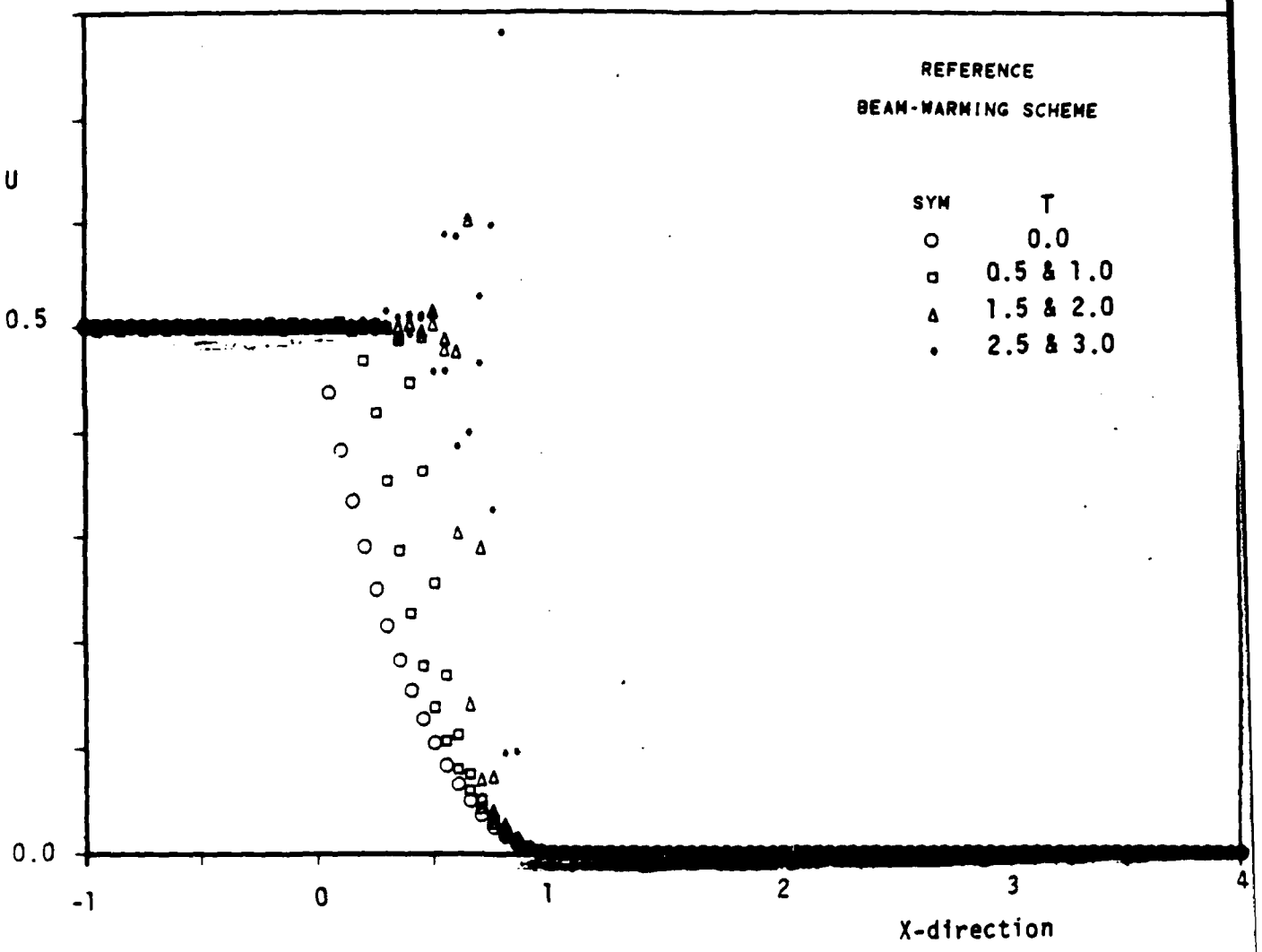

FIGURE 6: "Numerical solution of Burgers' equation in Quasi-Linear form using Beam-Warming's implicit method."

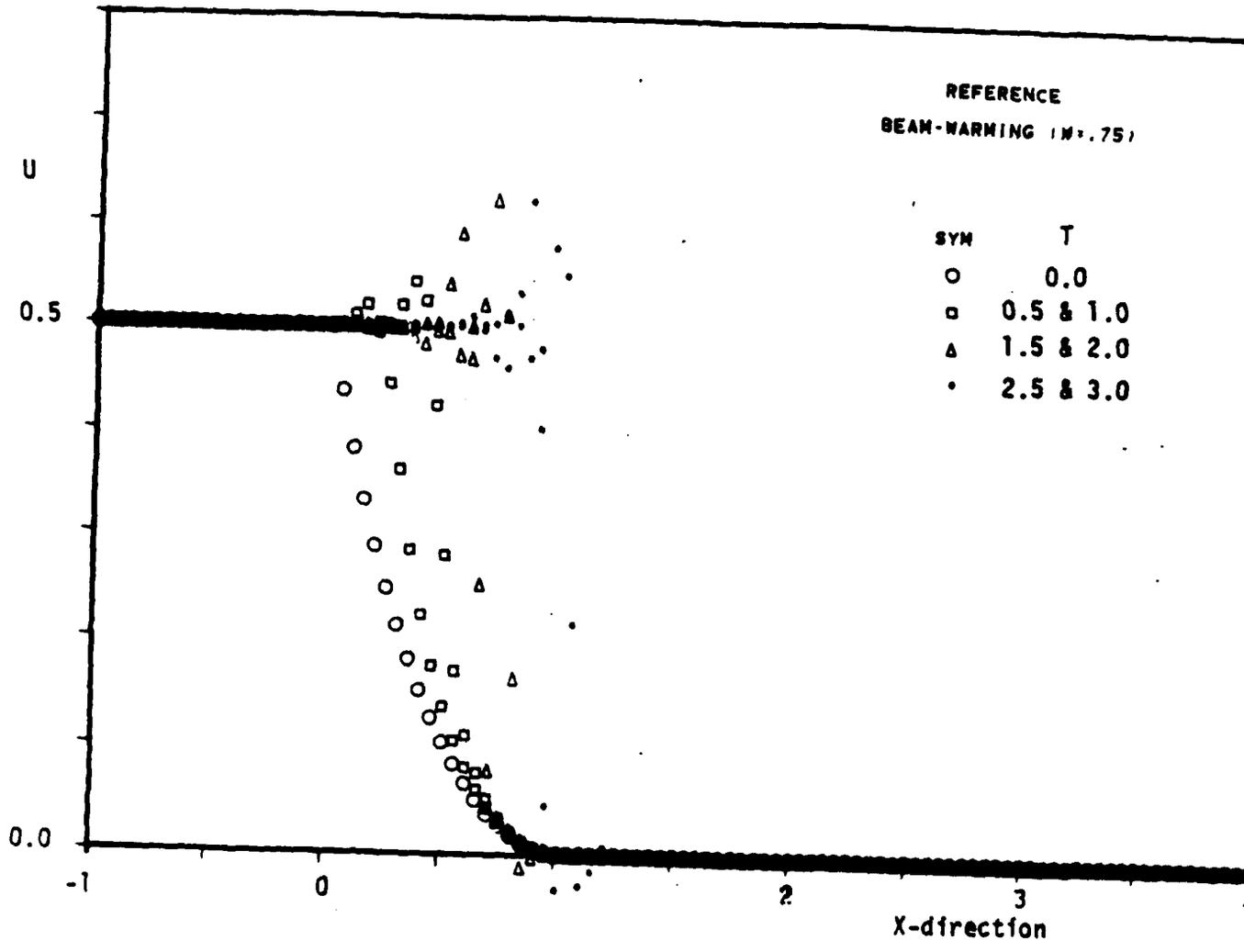

FIGURE 7: "Numerical solution of Burgers' equation in Fully-Conservative form using Beam-Warming's method with dissipation."

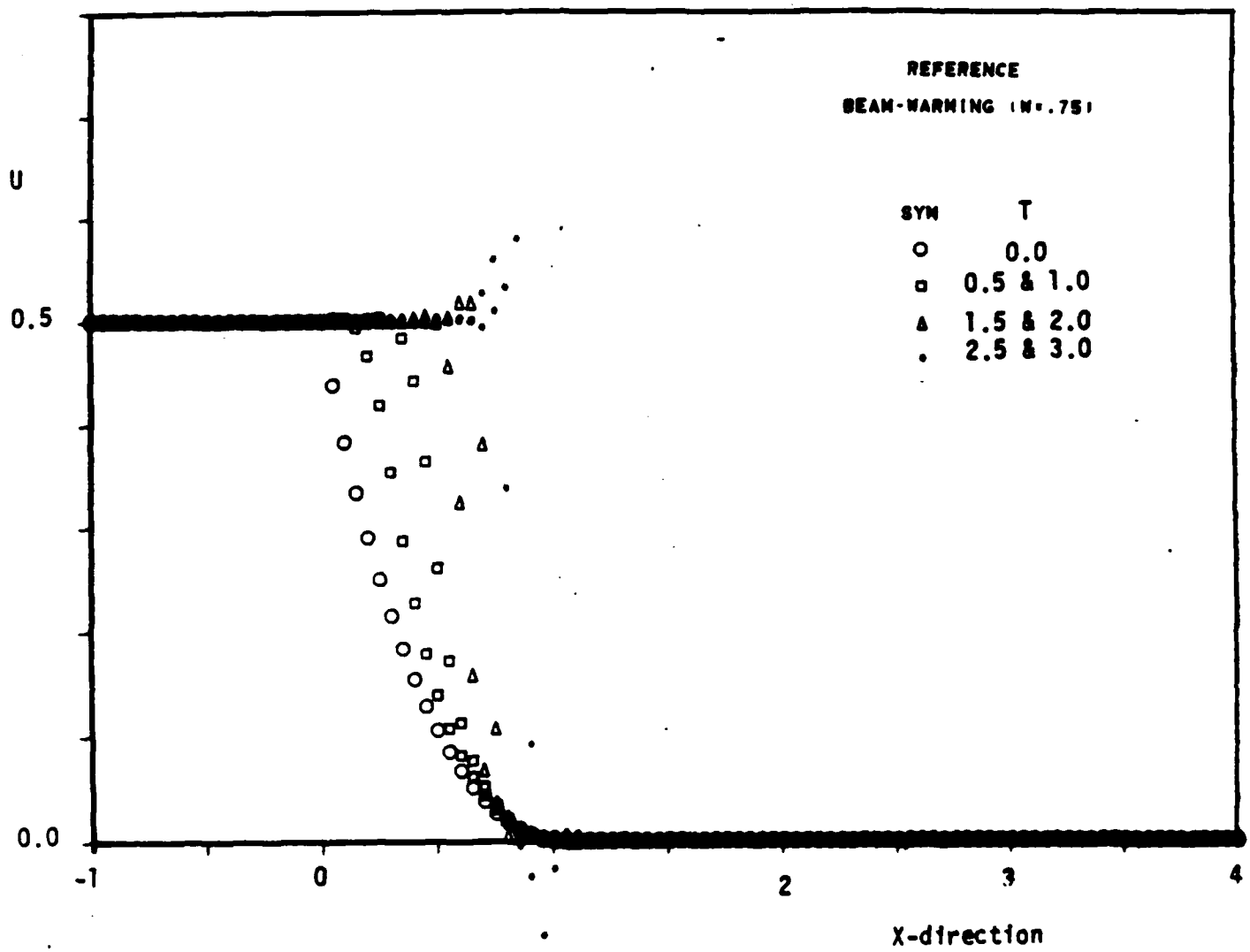

FIGURE 8: "Numerical solution of Burgers' equation in Quasi-Linear form using Beam-Warming's method with dissipation."

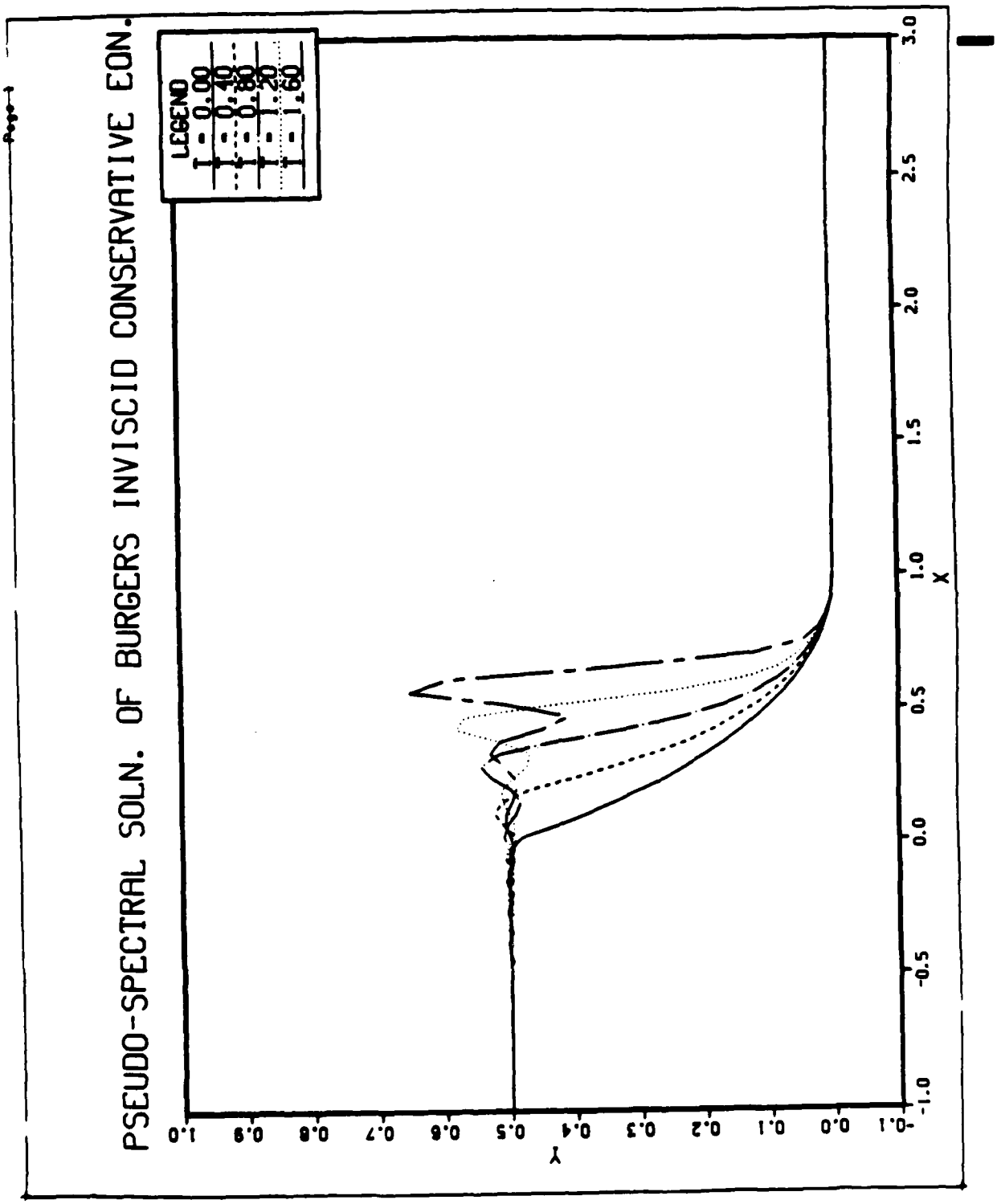

FIGURE 9: "Numerical solution of Burgers' equation in Fully-Conservative form using the Pseudo-Spectral method."

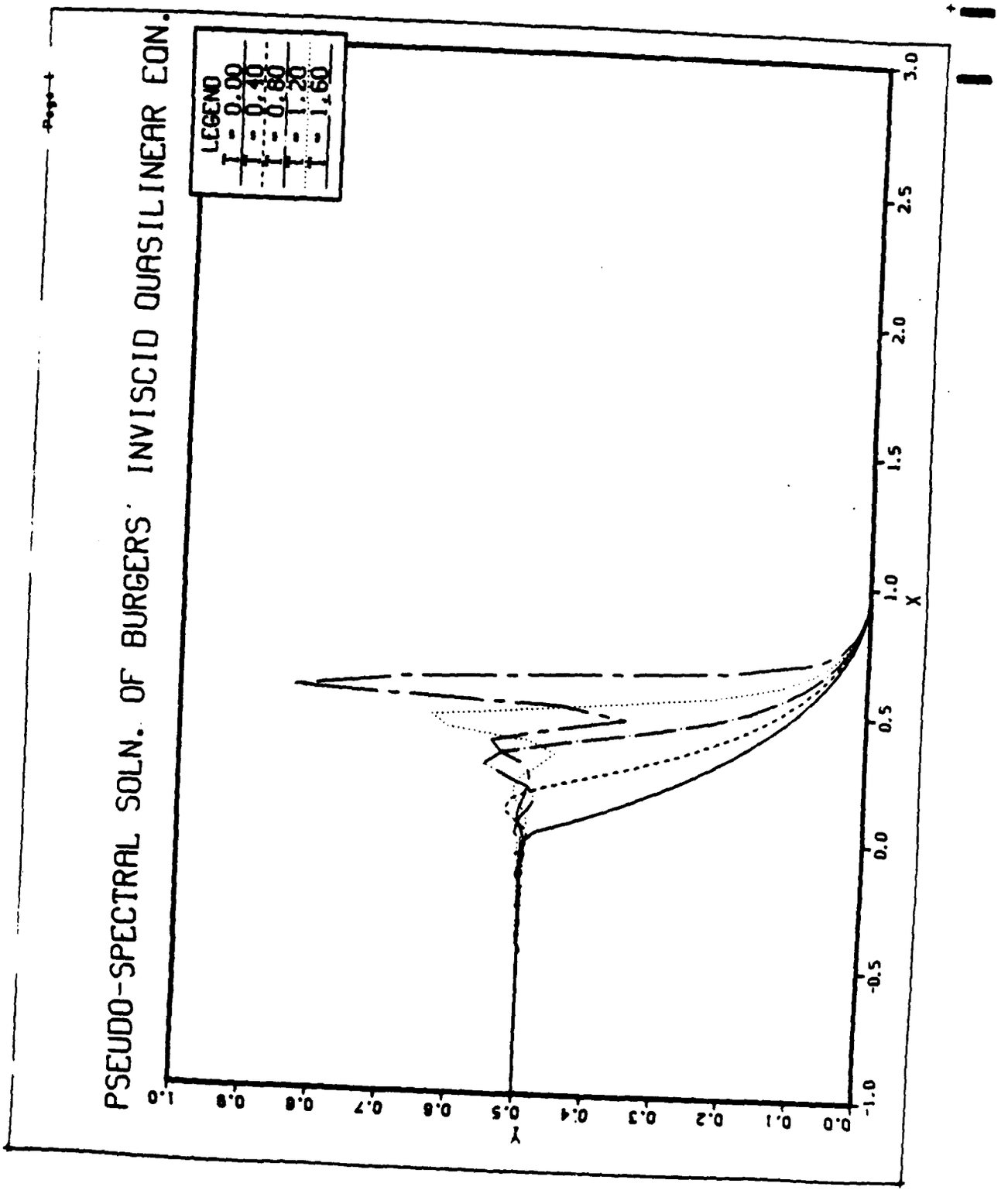

FIGURE 10: "Numerical solution of Burgers' equation in Quasi-Linear form using the Pseudo-Spectral method."

END

1-87

DTIC